Dyes and Pigments 80 (2009) 130–135

Contents lists available at ScienceDirect

Dyes and Pigments

journal homepage: www.elsevier.com/locate/dyepig

The synthesis, cyclic voltammetry and spectroelectrochemical studies of Co(II) phthalocyanines tetra-substituted at the α and β positions with phenylthio groups

Nolwazi Nombona, Tebello Nyokong*

Department of Chemistry, Rhodes University, Grahamstown 6140, South Africa

ARTICLE INFO

Article history:
Received 24 April 2008
Received in revised form 1 June 2008
Accepted 2 June 2008
Available online 10 June 2008

Keywords:
Cobalt phthalocyanine
Cyclic voltammetry
Spectroelectrochemistry
Peripheral
Reduction
Oxidation

ABSTRACT

Non-peripherally substituted cobalt 1,(4)-(tetraphenylthiophthalocyaninato) and peripherally substituted cobalt 2,(3)-(tetraphenylthiophthalocyaninato) complexes were synthesized. Redox processes were observed at $E_{1/2} = -1.44$ V (I), -0.39 V (II), $+0.37$ V (III), $+0.78$ V (IV) and 1.15 V (V) for the non-peripherally substituted and at $E_{1/2} = -1.42$ V (I), -0.57, -0.39 V (II), $+0.27$ V (III), $+0.79$ V (IV) and $+1.10$ V (V) for the peripherally substituted complexes, respectively. The couples were assigned to $Co^{I}Pc^{-2}/Co^{I}Pc^{-3}$ (I), $Co^{II}Pc^{-2}/Co^{I}Pc^{-2}$ (II), $Co^{III}Pc^{-2}/Co^{II}Pc^{-2}$ (III), and $Co^{III}Pc^{-1}/Co^{III}Pc^{-2}$ (IV) using spectroelectrochemistry. The last process (V) could not be ascertained by spectroelectrochemistry but is associated with ring oxidation. Upon reduction or oxidation, the Q band of the non-peripherally substituted complex became less red shifted compared to that of its peripherally substituted counterpart.

© 2008 Elsevier Ltd. All rights reserved.

1. Introduction

Metallophthalocyanines (MPcs) are used in a number of applications due to their increased stability, architectural flexibility, diverse coordination properties and improved spectroscopic characteristics. Applications in fields such as chemical sensors [1–3], liquid crystals [4,5], semiconductors [6], non-linear optics [7,8] and photodynamic therapy (PDT) [9,10] have shown increased importance of these macrocycles. Their physicochemical properties can be fine-tuned by changing the metal and/or nature of substituents. The positions of the absorption bands in phthalocyanines (particularly the Q band) are affected to a varying degree by the central metal, axial ligation, solvents, peripheral and non-peripheral substitution, aggregation and by extension of the conjugation. Pcs with sulphur substituents, in particular, are highly red shifted and have found applications in energy conversion and optical devices [11]. The effect of the central metal in MPc complexes on the absorption spectra is usually small except for a few metals such as Mn, Sb, Bi and V. In some cases MPcs containing central metals such as Zn, show red shift due to the deformation of the methoxyphenyl substituents [12]. In this ZnPc derivative, the HOMO–LUMO gap was narrowed due to the destabilization of the HOMO caused by increased electrostatic repulsion between carbon atoms at the non-peripheral positions and the electron-rich methoxyphenyl substituents. Non-peripheral substitution by bulky groups results in steric hindrance of substituents at the 1,4-position of the adjacent benzene ring. In our continuing research on the development of thio substituted MPc complexes for development of self-assembled monolayers (SAMs) and for applications requiring red-shifted absorption spectra, this work reports on CoPc complexes substituted at the peripheral (β) or non-peripheral (α) positions. CoPc complexes are very well known for their excellent electrocatalytic properties.

The electrochemistry of MPc complexes containing sulphur substituents often show complicated electrochemistry involving the central metal, the Pc ring and the Pc ring substituents, hence elucidation of the electrochemical behaviour of thio substituted derivatives is of interest, hence in the work, electrochemical and spectroelectrochemical behaviours of CoPc complexes shown in Scheme 1 are presented. The complexes are cobalt 1,(4)-(tetraphenylthiophthalocyaninato) (**5**) and cobalt 2,(3)-(tetraphenylthiophthalocyaninato) (**6**). The effects of α versus β substitution on the electrochemistry are discussed.

---

* Corresponding author. Tel.: +27 46 6038260; fax: +27 46 6225109.
E-mail address: t.nyokong@ru.ac.za (T. Nyokong).

0143-7208/$ – see front matter © 2008 Elsevier Ltd. All rights reserved.
doi:10.1016/j.dyepig.2008.06.002

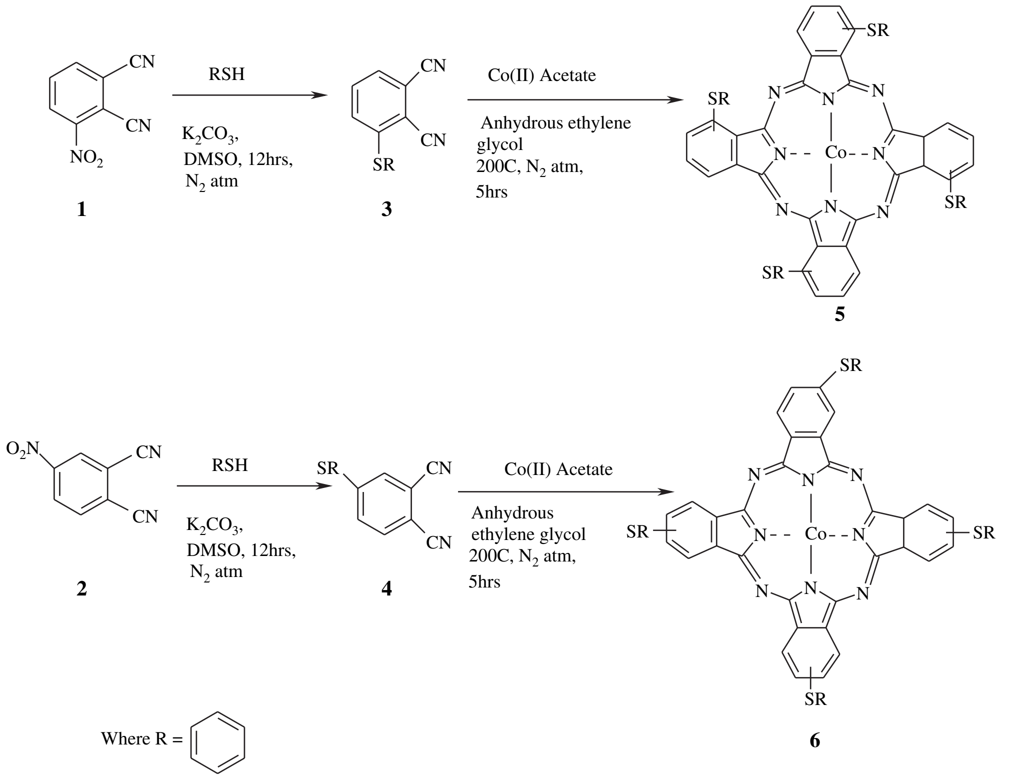

Scheme 1. Synthesis of CoPc derivatives: cobalt 1,(4)-(tetraphenylthiophthalocyaninato) (**5**) and cobalt 2,(3)-(tetraphenylthiophthalocyaninato) (**6**). Complexes **7** (α) and **8** (β) are the same as above except Co(II) is replaced by OTi(IV).

2. Results and discussion

2.1. Synthesis and characterization

Both complexes **5** and **6** were characterized using UV–vis, IR and elemental analysis and they gave satisfactory results confirming the purity of the complexes. The IR spectra of the complexes gave vibrational peaks at 668 cm^{-1} for **5** and 686 cm^{-1} for **6**, confirming the presence of a C–S–C stretch. Fig. 1 shows the UV–vis spectra of the synthesized complexes. Complex **5** has a Q-band absorption at 695 nm whereas complex **6** has a Q-band absorption at 673 nm. The 22 nm red shift observed for complex **5** is due to the electron density enhancement caused by the substitution at the non-peripheral (α) position. It is well known that α substitution results in red shifting of the spectra in MPc complexes [13,14]. The 22 nm red shift is smaller than the 32 nm red shift observed for the corresponding (O)TiPc complexes [15], thus showing the central metal also plays a role in the extent of red shifting of the Q band in MPc complexes.

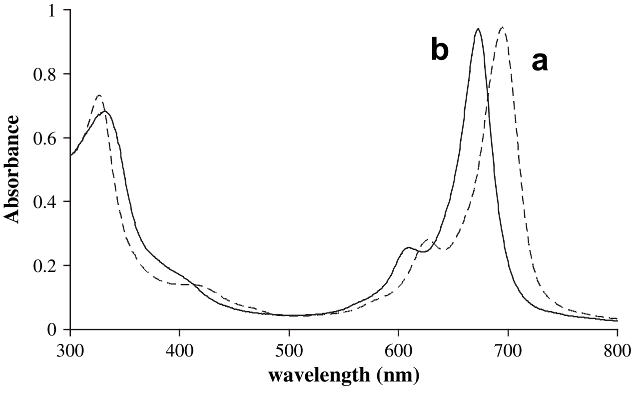

Fig. 1. UV–vis absorption spectra in DMF of complex (a) **5** and (b) **6**. Concentration ~1 × 10^{-6} M.

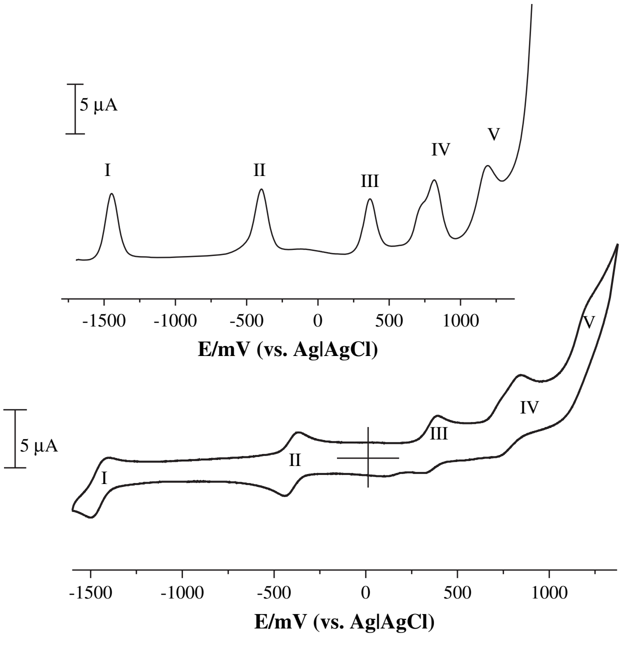

Fig. 2. Cyclic (bottom) and square wave (top) voltammograms of complex **5**. Medium = DMF containing 0.1 M TBABF$_4$. Scan rate = 100 mV s^{-1}.

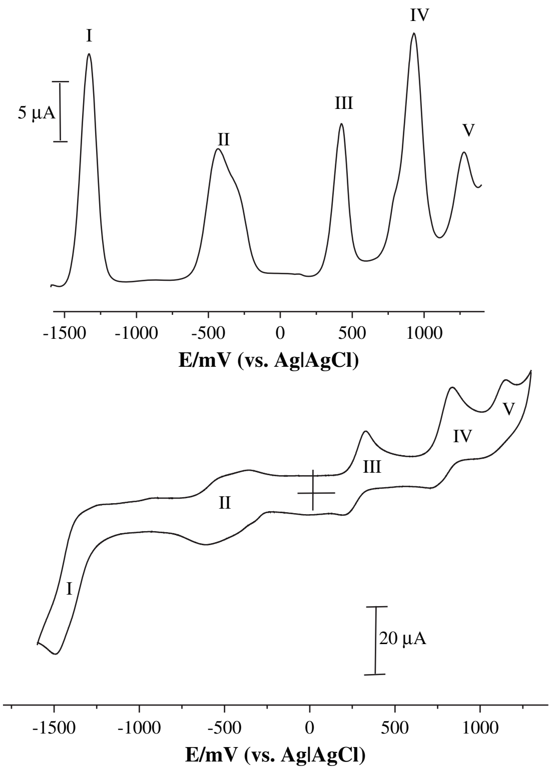

Fig. 3. Cyclic (bottom) and square wave (top) voltammograms of complex **6**. Medium = DMF containing 0.1 M $TBABF_4$. Scan rate = 100 mV s^{-1}.

Aggregation is usually depicted as a coplanar association of rings progressing from monomer to dimer and higher order complexes. In this study, the aggregation behaviour of the phthalocyanines **5** and **6** was investigated at different concentrations in DMF. As the concentration was increased, the intensity of absorption of the Q band also increased and there were no new bands (normally blue shifted) due to the aggregated species. Beer–Lambert law was obeyed for both complexes in DMF for concentrations less than 1×10^{-5} mol dm^{-3}.

2.2. Cyclic voltammetry

Cyclic voltammetry and square wave voltammetry experiments were performed for the synthesized complexes in DMF using a glassy carbon electrode as the working electrode. Figs. 2 and 3 show cyclic and square wave voltammograms of complexes **5** and **6**, respectively. Within the −1500 mV to +1400 mV potential window two reductions and three oxidations are observed. Complex **5** shows redox processes at $E_{1/2} = -1.44$ V (I), −0.39 V (II), +0.37 V (III), +0.78 V (IV) and 1.15 V (V) versus Ag|AgCl. Processes I and II are reversible with anodic to cathodic peak separation (ΔE) of 60 mV and 80 mV (ΔE value for the ferrocene standard was 85 mV), respectively, and the ratio of anodic to cathodic peak currents of near unity. Processes III and IV are quasi-reversible in that both had weak cathodic peaks (even though ΔE for III was 60 mV). Square wave voltammogram shows that process IV is split. The split is not very clear in the cyclic voltammogram. The splitting could be due to some degree of aggregation as explained below for complex **6**. Process V is near the limits of the medium and electrode, hence is not well resolved. When a narrower scan window (between +1000 mV and −1000 mV) was employed for complex **5**, there was not much improvement in the reversibility of processes III and IV, confirming that observed behaviour is not due to the use of the limits of the system. Ring oxidation of alkylthio substituted MPc complexes often results in decomposition [16] hence the lack of reversibility of the oxidation processes is not surprising.

For complex **6** the redox processes (Fig. 3) were observed at $E_{1/2} = -1.42$ V (I), −0.57, −0.39 V (II), +0.27 V (III), +0.79 V (IV) and +1.10 V (V) versus Ag|AgCl. All processes are not completely reversible in terms of both ΔE and the ratio of anodic to cathodic peak currents. In addition process II showed a complicated behaviour consisting of overlapping peaks. Such behaviour is usually associated with aggregation in MPc complexes [17]. Using a narrower range did not improve the behaviour of couple II, however, the cathodic currents of process III improved.

The difference in the behaviour of couple II for the two complexes could be related to the fact that substitution at the non-peripheral positions prevents aggregation more than at the peripheral positions, hence complex **5** (non-peripherally substituted) shows less complicated behaviour than **6** (peripherally substituted). Process IV showed some splitting for both complexes, which is seen most clearly using square wave voltammetry. The effects of aggregation will be pronounced for cyclic voltammetry due to the high concentrations ($\sim 10^{-3}$ M) employed compared to UV–vis spectra (Fig. 1), where low concentrations ($\sim 1 \times 10^{-6}$ M) are used. Comparing the cyclic voltammograms of complexes **5** and **6** with those of corresponding OTiPc, Table 1, reveals that there was no ring oxidation in the latter. OTiPc derivatives will be easier to reduce and difficult to oxidize due to the electropositive nature of the Ti(IV) central metal.

Process V may be due to the oxidation of the thio substituents on the ring in addition to the ring itself, for both complexes, this and the fact that the electrode is at its limit may explain why this peak appears to be smaller compared to the other peaks.

2.3. Spectroelectrochemistry

Spectroelectrochemistry was performed using an optically transparent thin-layer electrode (OTTLE) cell in order to determine the nature of the redox processes occurring. Fig. 4(a) shows the spectral changes observed when the reduction potential for couple II (complex **5**) was applied, there was a shift of the Q band from 695 nm to 726 nm and a new band was formed near 482 nm. The latter band is a characteristic of $Co^{I}Pc^{-2}$complexes [14]. Thus the

Table 1
Cyclic voltammetry data for complexes **5** and **6** and the corresponding OTiPc complexes: oxotitanium 1,(4)-(tetraphenylthiophthalocyaninato) (**7**) and oxotitanium 2,(3)-(tetraphenylthiophthalocyaninato) (**8**). Electrolyte: DMF containing $TBABF_4$

Complex	$E_{1/2}$ (V versus Ag|AgCl)					
	I ($Co^{I}Pc^{-2}/Co^{I}Pc^{-3}$) or ($Ti^{II}Pc^{-2}/Ti^{II}Pc^{-3}$)	II ($Co^{II}Pc^{-2}/Co^{I}Pc^{-2}$) or ($Ti^{III}Pc^{-2}/Ti^{II}Pc^{-2}$)	($Ti^{IV}Pc^{-2}/Ti^{III}Pc^{-2}$)	III ($Co^{III}Pc^{-2}/Co^{II}Pc^{-2}$)	IV ($Co^{III}Pc^{-1}/Co^{III}Pc^{-2}$)	V ($Co^{III}Pc^{0}/Co^{III}Pc^{-1}$)
5	−1.44	−0.39		+0.37	+0.78	+1.15
6	−1.42	−0.57, −0.39		+0.27	+0.79	+1.10
7[a]	−1.33	−0.46	−0.07			
8[a]	−1.20	−0.37	−0.07			

[a] Data from Ref. [15].

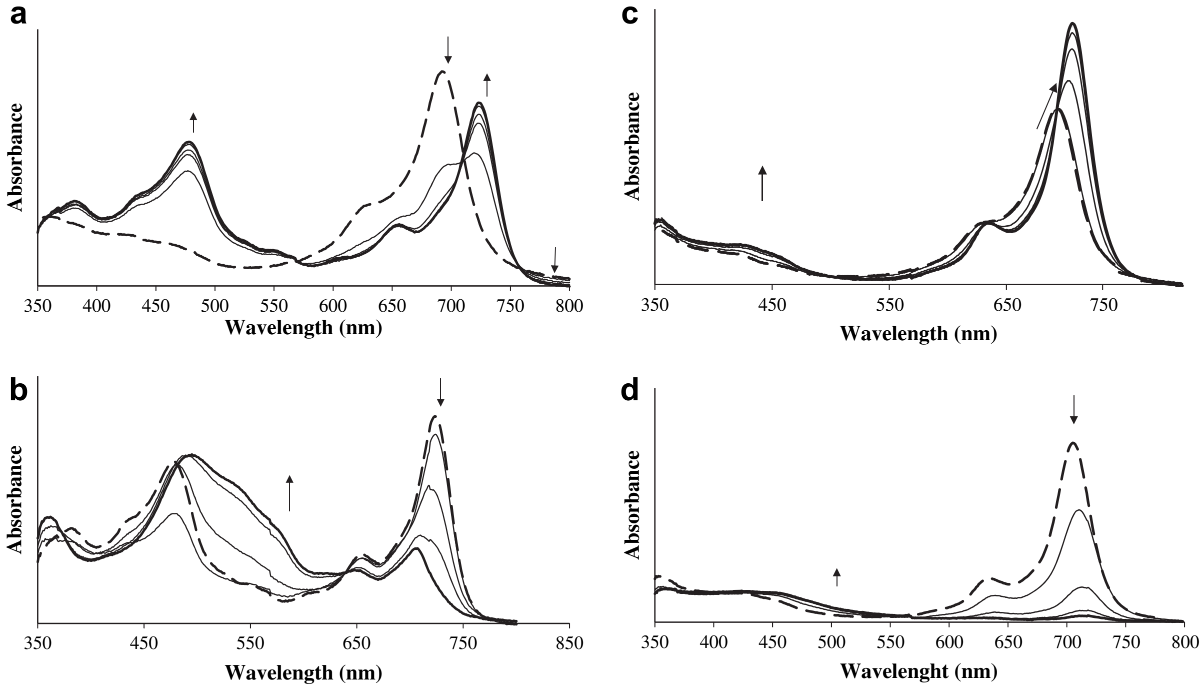

Fig. 4. UV–vis spectral changes of complex **5** in DMF containing 0.1 M $TBABF_4$ observed during application of controlled potential at potentials of the following processes: (a) II (−0.5 V), (b) I (−1.5 V), (c) III (+0.4 V) and (d) IV (+0.8 V). The first scan in (b) is the same as the last scan in (a). The first scan in (d) is the same as the last scan in (c).

presence of this band coupled to the shifting of the Q band to low energy, is a typical behaviour for the formation of $Co^{I}Pc^{-2}$ species [14]. Clear isosbestic points observed at 756 nm, 710 nm and 547 nm confirmed the presence of only two species. When the potential was increased to reduction potentials for couple I, Fig. 4(b), there was a drastic decrease in Q-band absorbance at 726 nm with a simultaneous increase of absorption between 480 nm and 636 nm, typical of ring reduction in MPc complexes [18,19] forming $Co^{I}Pc^{-3}$. The absorption band at 482 nm shifted to 497 nm and the Soret band from 387 nm to 365 nm following the reduction at potentials of process I. An isosbestic point was observed at 636 nm. The original species could be completely regenerated upon application of 0 V following reduction at potentials for couples I and II, confirming the reversible nature of the couples.

Oxidation of the complex at potentials of couple III in Fig. 4(c) showed a shifting of the Q band from 695 nm to 709 nm, with an isosbestic point at 693 nm. The shift in the Q band accompanied by an increase in intensity is a typical behaviour [14] for the formation of the $Co^{III}Pc^{-2}$, thus couple III is assigned to $Co^{II}Pc^{-2}/Co^{III}Pc^{-2}$. Further oxidation at the potentials of process IV in Fig. 3(d) showed the spectral changes typical of ring-based processes, there was a large decrease in the absorbance of the Q band with an isosbestic points at 522 nm and a broad band near 500 typical [18,19] of ring oxidation, hence confirming that process IV is due to $Co^{II}Pc^{-2}/Co^{II}Pc^{-1}$. The regeneration of original species (∼50%) could be observed by reversal of the applied potential for couple IV, confirming the lack of complete reversibility of this process. Applications of oxidation potentials of process V continued the degradation process. For all processes for complex **5**, the number of electrons transferred was calculated using the equation $Q = nFVC$ and n was found to be close to one.

Spectroelectrochemical studies on complex **6** were also carried out in order to assign the cyclic voltammetry peaks. Reduction at potentials of couple II resulted in reduction in intensity and a hypsochromic shift of the Q band from 673 nm to 711 nm (Fig. 5(a)) with a simultaneous increase of the band at 478 nm. These spectral changes are typical for the formation of $Co^{I}Pc^{-2}$ as discussed above for complex **5**. Isosbestic points were observed at 693 nm, 568 nm and 399 nm. The spectra could be regenerated to ∼80% on potential reversal following application of potential for couple II. Application of potential for couple I (figure not shown) resulted in a decrease in Q-band absorption intensity and an increase in absorption in the 500 nm region, as observed above for complex **5**, typical [18] of ring-based reduction process ($Co^{I}Pc^{-2}/Co^{I}Pc^{-3}$). When the oxidation potential for process III was applied, Fig. 5(b), a gradual redshifting of the Q band from 673 nm to 686 nm with increasing intensity was observed. Isosbestic points were observed at 507 nm and 681 nm, these spectral changes confirm a metal based oxidation process to form the $Co^{III}Pc^{-2}$ species. Increasing the potential to values of couple IV, Fig. 5(c), resulted in a considerable decrease in Q-band absorption with a slight increase in absorption at 500 nm region, an isosbestic point was observed at 530 nm. The weakness of the peak in 500 nm region shows possible degradation of the complex. The spectra could be regenerated to ∼50% on potential reversal following application of potential for couple IV, showing the lack of complete reversibility of this process observed in the cyclic voltammogram. Again applications of potentials of process V continued the degradation process.

Table 2 lists the main absorbance peaks for oxidized and reduced species for complexes **5** and **6**. Only the metal based processes are shown in Table 1 and are compared to those reported for the corresponding OTiPc. As stated above, the presence of the thio substituents at the non-peripheral position for complex **5**, results in a red shift of 22 nm compared to peripheral substitution in complex **6**. The red shifting of the Q band is due to the destabilization of the highest occupied molecular orbital (HOMO) in MPc complexes relative to the lowest unoccupied molecular orbital (LUMO) [20]. Upon oxidation or reduction of the central Co(II) metal to Co(III) or Co(I), respectively, the red shifting of the Q band of complex **5** relative to **6**, decreased to 13 nm and 15 nm (Table 2). Thus it seems the extent of destabilization of the HOMO is also dependent on the

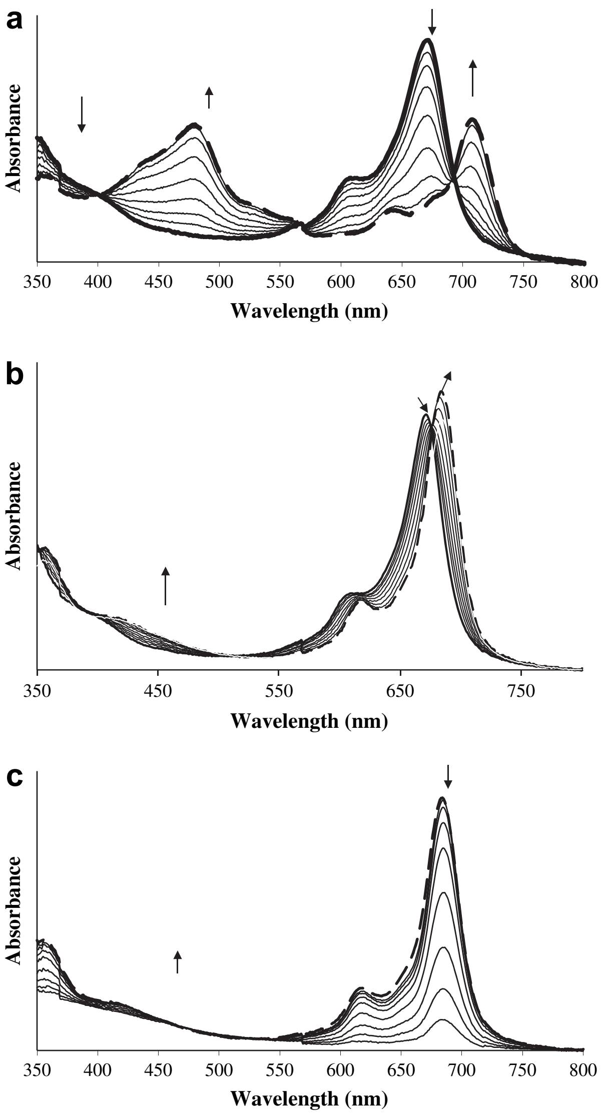

Fig. 5. UV–vis spectral changes of complex **6** in DMF containing 0.1 M $TBABF_4$ observed during application of controlled potential at potentials of the following processes: (a) II (−0.6 V), (b) III (+0.4 V) and (c) IV (+0.8 V). The first scan in (c) is the same as the last scan in (b).

oxidation state of the central metal. Similar decrease in red shifting of the Q band of the non-peripherally substituted (relative to peripherally substituted) complexes was also observed for the corresponding OTiPc, where the red shift decreased from 32 nm for Ti(IV) to 7 nm for Ti(III) and 14 nm for Ti(II) phthalocyanine complexes, Table 2.

Table 2
Main absorption bands for complexes **5** and **6** and the corresponding OTiPc complexes: oxotitanium 1,(4)-(tetraphenylthiophthalocyaninato) (**7**) and oxotitanium 2,(3)-(tetraphenylthiophthalocyaninato) (**8**) in DMF

Complex	Q-band absorption (nm)		
	$Co^{III}Pc^{-2}$	$Co^{II}Pc^{-2}$	$Co^{I}Pc^{-2}$
5	709	695	726, 477
6	686	673	711, 478
	$OTi^{IV}Pc^{-2}$	$OTi^{III}Pc^{-2}$	$OTi^{II}Pc^{-2}$
7[a]	744	710	706
8[a]	712	703	694

[a] From Ref. [15].

Based on the cyclic voltammetry and spectroelectrochemistry data, the redox processed (I–IV) for both complexes (**5** and **6**) are assigned as shown in Eqs. (1)–(4):

$$Co^{I}Pc^{-2} + e^{-} \rightarrow Co^{I}Pc^{-3} \quad \text{(process I)} \tag{1}$$

$$Co^{II}Pc^{-2} + e^{-} \rightarrow Co^{I}Pc^{-2} \quad \text{(process II)} \tag{2}$$

$$Co^{II}Pc^{-2} \rightarrow Co^{III}Pc^{-2} + e^{-} \quad \text{(process III)} \tag{3}$$

$$Co^{III}Pc^{-2} \rightarrow Co^{III}Pc^{-1} + e^{-} \quad \text{(process IV)} \tag{4}$$

3. Experimental

3.1. Materials

3-Nitrophthalonitrile (**1**), 4-nitrophthalonitrile (**2**), 3-phenylthiophthalonitrile (**3**) and 4-phenylphthalonitrile (**4**) were synthesized as reported in literature [15]. Anhydrous ethylene glycol, potassium carbonate, cobalt(II) acetate and tetrabutylammonium tetrafluoroborate ($TBABF_4$) were purchased form Sigma–Aldrich. Dimethylsulfoxide (DMSO) and dimethylformamide (DMF) were from Saarchem. Silica gel for column chromatography was purchased from MERK. All solvents used for electrochemical experiments were freshly distilled and deaerated by bubbling argon before use and the electrochemical set-up was kept under argon atmosphere throughout the experiments, other reagents were used as received.

3.2. Equipment

UV–vis absorption spectra were obtained using the Varian 500 UV–vis–NIR spectrophotometer. IR spectra (KBr pellets) were obtained by using the Perkin–Elmer 2000 FT-IR spectrometer. Elemental analysis was performed at the University of Cape Town, South Africa, using a Thermo Flash EA 1112 series elemental analyzer.

3.3. Electrochemical methods

Cyclic voltammetry (CV) and square wave voltammetry (SWV) experiments for the characterization of the cobalt phthalocyanine complexes were carried out using the B/W 100 Electrochemical Workstation. A three electrode set-up was employed consisting of a glassy carbon electrode (GCE, 3.0 mm diameter) as the working electrode, Ag|AgCl wire pseudo-reference electrode and a platinum wire counter electrode. The potential response of Ag|AgCl pseudo-reference in aqueous conditions was less than the Ag|AgCl (3 M KCl) by 0.015 ± 0.003 V. The SWV settings were: step potential = 4 mV, pulse height = 25 mV, pulse frequency = 15 Hz. Spectroelectrochemical experiments were conducted using a home-made optically transparent thin-layer electrochemical (OTTLE) cell connected to a Bio analytical system (BAS) CV 27 voltammogram.

3.4. Synthesis

The synthetic route followed in this work is shown in Scheme 1.

3.4.1. Synthesis of 1,(4)-(tetraphenylthiophthalocyaninato) (*5*)

In anhydrous ethylene glycol (20.4 ml), 3-(phenylthio)phalonitrile (**3**) (2.55 g, 10.7 mmol) and cobalt(II) acetate (0.64 g, 2.68 mmol) were stirred under reflux in a nitrogen atmosphere at 200 °C for 5 h. The reaction mixture was left to cool to room temperature, thereafter methanol (30 ml) was added to precipitate out the dark green crude product. The mixture was filtered and treated in a Soxhlet extraction apparatus with ethanol for 48 h. The product was further purified by column chromatography, using THF as the eluting solvent. After evaporation of the solvent, the product was purified further by washing twice in methanol and lastly in acetone, to give a pure dark green product. Yield: 36%. UV–vis (DMF): λ_{max} nm (log ε) 326 (4.15), 626 (4.56), 693 (4.71). IR [(KBr)ν_{max}/cm^{-1}]: 668 (C–S–C). Calcd. for $C_{56}H_{32}N_8OS_4Co$: C, 66.98; H, 3.21; N, 11.16; Found: C, 66.17; H, 3.20; N, 10.65.

*3.4.2. Synthesis of cobalt 2,(3)-(tetraphenylthiophthalocyaninato) (**6**)*

Synthesis and purification of **6** were the same as for **5** except **4** instead of **3** was used. Yield: 40%. UV–vis (DMF): λ_{max} nm (log ε) 331 (4.03), 608 (4.51), 671 (4.66). IR [(KBr)ν_{max}/cm^{-1}]: 686 (C–S–C). Calcd. for $C_{56}H_{32}N_8OS_4Co$: C, 66.98; H, 3.21; N, 11.16; Found: C, 66.68; H, 3.36; N, 10.33.

4. Conclusions

In conclusion, complexes **5** and **6** containing thiophenyl substituents at the non-peripheral and peripheral positions, respectively, show similar cyclic voltammogram behaviour, however, complex **6** showed more complicated redox behaviour. Using spectroelectrochemistry, the cyclic voltammetry peaks were assigned to $Co^{I}Pc^{-2}/Co^{I}Pc^{-3}$ (I), $Co^{II}Pc^{-2}/Co^{I}Pc^{-2}$ (II), $Co^{III}Pc^{-2}/Co^{II}Pc^{-2}$ (III), and $Co^{III}Pc^{-1}/Co^{III}Pc^{-2}$ (IV). The red shifting of the Q band of the non-peripherally substituted (relative to the peripherally substituted) derivatives was found to decrease on reduction or oxidation at the central metal.

Acknowledgements

This work was supported by the Department of Science and Technology (DST) and National Research Foundation (NRF), South Africa through DST/NRF South African Research Chairs Initiative for Professor of Medicinal Chemistry and Nanotechnology as well as Rhodes University. NN thanks Andrew Mellon foundation and NRF for scholarships.

References

[1] Guillaud G, Simon J, Germain JP. Coord Chem Rev 1998;178–180:1433.
[2] Collins RA, Mohammed KA. J Phys D Appl Phys 1988;21:154.
[3] Zagal J, Bedioui F, Dodelet JP, editors. N4-macrocyclic metal complexes. New York: Springer; 2006.
[4] McKeown NB. Chem Ind 1999:92.
[5] Duro AJ, de la Torre G, Barber J, Serrano JL, Torres T. Chem Mater 1996;8:1061.
[6] Classens CG, Blau WJ, Cook M, Hanack M, Nolte RJM, Torres T, et al. Monatsh Chem 2001;132:3.
[7] de la Torre G, Vasquez P, Agulló-Ĺopez F. Adv Mater 1997;9:265.
[8] de la Torre G, Vaquez P, Agulló-Ĺopez F, Torres T. J Mater Chem 1998;8:1671.
[9] Allen CM, Sharman WM, van Lier JE. J Porphyrins Phthalocyanines 2001;5:1.
[10] Bonnett R. In: Chemical aspects of photodynamic therapy. Canada: Gordon and Breach Science; 2000.
[11] Gregory P. J Porphyrins Phthalocyanines 2000;4:432.
[12] Fukuda T, Ishiguro I, Kobayashi N. Tetrahedron Lett 2005;46:2907.
[13] Nyokong T, Isago H. J. Porphyrins Phthalocyanines 2004;8:1083.
[14] Stillman MJ, Nyokong T. In: Leznoff CC, Lever ABP, editors. Phthalocyanines: properties and applications, vol. 1. New York: VCH; 1989 [chapter 3].
[15] Tau P, Nyokong T. Dalton Trans 2006:4482.
[16] Takahashi K, Kawashima M, Tomita Y, Itoh M. Inorg Chim Acta 1995;232:69.
[17] Lever ABP, Milaeva ER, Speier G. In: Leznoff CC, Lever ABP, editors. Phthalocyanines: properties and applications, vol. 3. New York: VCH Publishers; 1993.
[18] Stillman MJ. In: Leznoff CC, Lever ABP, editors. Phthalocyanines: properties and applications, vol. 3. New York: VCH Publishers; 1993 [chapter 5].
[19] Mark J, Stillman MJ. In: Kadish KM, Smith KM, Guilard R, editors. Porphyrin handbook. Phthalocyanines: spectroscopic and electrochemical characterization, vol. 16. New York: Academic Press; 2003.
[20] Kobayashi N, Konami H. Phthalocyanines: properties and applications, vol. 4. New York: VCH; 1999.